

JAERI-M
82-048

MATHEMATICAL SIMULATION OF FALLING
LIQUID FILM CONDENSER FOR REMOVAL
OF HELIUM AND SEPARATION OF
HYDROGEN ISOTOPES

May 1982

Masahiro KINOSHITA, John R. BARTLIT*
and Robert H. SHERMAN*

日本原子力研究所
Japan Atomic Energy Research Institute

JAERI-M レポートは、日本原子力研究所が不定期に公刊している研究報告書です。

入手の間合わせは、日本原子力研究所技術情報部情報資料課（〒319-11 茨城県那珂郡東海村）あて、お申しこしてください。なお、このほかに財団法人原子力弘済会資料センター（〒319-11 茨城県那珂郡東海村日本原子力研究所内）で複写による実費頒布をおこなっております。

JAERI-M reports are issued irregularly.

Inquiries about availability of the reports should be addressed to Information Section, Division of Technical Information, Japan Atomic Energy Research Institute, Tokai-mura, Naka-gun, Ibaraki-ken 319-11, Japan.

© Japan Atomic Energy Research Institute, 1982

編集兼発行 日本原子力研究所
印刷 山田軽印刷所

Mathematical Simulation of Falling Liquid Film Condenser
for Removal of Helium and Separation of Hydrogen Isotopes

Masahiro KINOSHITA, John R. BARTLIT* and Robert H. SHERMAN*

Division of Thermonuclear Fusion Research,
Tokai Research Establishment, JAERI

(Received April 27, 1982)

The present paper reports the extension of our previously reported work on mathematical simulation of a falling liquid film condenser. The mathematical model is fully described and its convergence characteristics are explored in detail. More concise parametric studies are made considering the low tritium concentration in the top gas the first priority desired.

The gas mixture of 50-50 D-T containing 1 % H and 5 % He is continuously fed to a point near the lower end of the sufficiently long packed section and separated into two streams : the helium gas containing ~ 10 % H₂-HD, and the liquid hydrogen isotopes containing 0.01 ppm He. The operating pressure is about 5 atm.

KEYWORDS : Isotope Separation, Hydrogen Isotopes, Helium,
Falling Liquid Film, Condenser, Mathematical Model,
Packed Section, Operating Pressure

* Los Alamos National Laboratory

ヘリウム除去及び水素同位体分離のための
流下液膜式凝縮器の数学的シミュレーション

日本原子力研究所東海研究所核融合研究部

木下正弘・John R. BARTLIT*・Robert H. SHERMAN*

(1982年4月27日受理)

本報告書は、先に我々が発表した、流下液膜式凝縮器の数学的シミュレーションに関する研究の拡充を図ったものである。数学的モデルが詳細に述べられ、シミュレーション手法の収束性も十分に調べられている。塔頂を出るヘリウムガス中のトリチウム濃度をキーパラメーターとして注目し、より詳細な特性解析が行われている。

1%のHと5%のHeを含むD-T混合ガスは、十分な長さを持った充填部の最下端付近に連続的に供給される。塔頂からは、約10%のH₂-HDを含むヘリウムガスが、塔底からは、Heを約0.01%しか含まない純度の高い水素同位体が連続的に取り出される。塔内操作圧力は約5 atmである。

* Los Alamos National Laboratory

CONTENTS

1.	Introduction	1
2.	Multi-dimensional Newton-Raphson Method	3
2.1	Convergence Method 1	5
2.2	Convergence Method 2	6
2.3	Convergence Method 3	7
3.	Mathematical Simulation Procedure for Falling Liquid Film Condenser	8
4.	Separation Characteristics	14
4.1	Distributions of Temperature, Phase Flows and Compositions ..	14
4.2	Effect of Operating Pressure	14
4.3	Convergence Characteristics	15
4.4	Effects of Number of Total Packed Stages and Total Amount of Heat Subtracted	16
4.5	Discussion on Uncertainty of Volatility of Helium	17
4.6	Addition of Protium to Feed Stream	18
5.	Conclusion	19
	NOMENCLATURE	20
	REFERENCES	22
	ACKNOWLEDGMENT	22

目 次

1. 序 論	1
2. 多変数ニュートンラフソン法	3
2.1 収束手法1	5
2.2 収束手法2	6
2.3 収束手法3	7
3. 流下液膜式凝縮器の数学的シミュレーション手順	8
4. 分離特性	14
4.1 温度, 流量及び組成分布	14
4.2 塔内操作圧力の影響	14
4.3 収束特性	15
4.4 充填部の理論段数及び冷却部からの全除去熱量の影響	16
4.5 ヘリウムの揮発度の不確定性	17
4.6 原料中へのHの添加	18
5. 結 論	19
記 号 表	20
参 考 文 献	22
謝 辞	22

1. Introduction

The falling liquid film condenser is a most attractive process for separation of helium from hydrogen isotopes. Figure 1 shows a conceptual flow diagram of a falling liquid film condenser.⁽¹⁾⁽²⁾ It is composed of the two sections, a cooled section and a packed section, and it has a heater at the bottom. The gas mixture of helium and hydrogen isotopes is continuously separated into two streams : a helium gas containing hydrogen isotopes which leaves the top of the column and a pure liquid hydrogen isotope stream free from helium which is withdrawn from the bottom. Heat subtraction is made from the cooled section through the column wall by the refrigerant (helium gas) which flows through the outer shell. As the gas flows up within the cooled section of the column, condensation of hydrogen isotopes proceeds and the liquid film formed by condensation falls along the column wall. As the liquid film flows down, liquid flows increase remarkably. The packed section where liquid flows are adequate, is located below. The main purpose of location of the packed section is promotion of hydrogen isotope separation. The helium gas from the top of the column is unavoidably accompanied by ~ 10 % hydrogen isotopes. Therefore, if the tritium concentration in the top gas is unacceptably high, the top gas must be processed by a tritium recovery system. However, promotion of hydrogen isotope separation using the packed section eliminates the need for the tritium recovery system, because the predominant molecular species of hydrogen

isotopes are H_2 and HD : the tritium concentration is sufficiently low and the top gas can be transferred to the tritium waste treatment system. This is the most attractive feature of the falling liquid film condenser.

The present study is the extension of our previously reported study.⁽¹⁾⁽²⁾ The mathematical simulation procedure is fully described and the convergence characteristics of the procedure are discussed in detail. More concise parametric studies are made considering the low tritium concentration in the top gas the first priority desired.

2. Multi-dimensional Newton-Raphson Method

The solution of a set of nonlinear simultaneous equations is the final step in the solution of simulation problems of the equilibrium stage processes such as cryogenic distillation columns, falling liquid film condensers and multistage-type water/hydrogen-exchange columns. These equations are expressed as the simultaneous zeroing of a set of functions (residual functions), where the number of functions to be zeroed is equal to the number of the independent variables.

Consider the following set of n nonlinear equations :

$$\left. \begin{aligned} f_1(x_1, \dots, x_n) &= 0 \\ &\vdots \\ f_n(x_1, \dots, x_n) &= 0 \end{aligned} \right\} . \quad (1)$$

By using the Taylor series expansion, we obtain

$$\begin{aligned} f_j(x_1 + \Delta x_1, \dots, x_n + \Delta x_n) &= f_j(x_1, \dots, x_n) + \\ &(\partial f_j / \partial x_1) \Delta x_1 + \dots + (\partial f_j / \partial x_n) \Delta x_n + \dots , \\ &(j = 1, \dots, n) . \end{aligned} \quad (2)$$

Assuming that the second and higher-order terms in the Taylor series expansion are sufficiently small, and $f_j(x_1 + \Delta x_1, \dots, x_n + \Delta x_n)$ is equal to zero, we obtain the following linear simultaneous equations with respect to Δx_j 's :

$$\left. \begin{aligned} (\partial f_1 / \partial x_1) \Delta x_1 + \dots + (\partial f_1 / \partial x_n) \Delta x_n &= -f_1 \\ &\vdots \\ (\partial f_n / \partial x_1) \Delta x_1 + \dots + (\partial f_n / \partial x_n) \Delta x_n &= -f_n \end{aligned} \right\} \quad (3)$$

The above equations can be written by

$$\Delta \vec{x} = - (\bar{G})^{-1} \vec{f} \quad , \quad (4)$$

where \vec{x} , $\Delta \vec{x}$ and \vec{f} are n-dimensional vectors defined by

$$\vec{x} = \begin{bmatrix} x_1 \\ \vdots \\ x_n \end{bmatrix} \quad , \quad \Delta \vec{x} = \begin{bmatrix} \Delta x_1 \\ \vdots \\ \Delta x_n \end{bmatrix} \quad \text{and} \quad \vec{f} = \begin{bmatrix} f_1 \\ \vdots \\ f_n \end{bmatrix} \quad , \quad (5)$$

respectively.

\bar{G} is the Jacobian matrix expressed by

$$\bar{G} = \begin{bmatrix} \partial f_1 / \partial x_1 & \dots & \partial f_n / \partial x_1 \\ \vdots & \ddots & \vdots \\ \partial f_n / \partial x_1 & \dots & \partial f_n / \partial x_n \end{bmatrix} \quad , \quad (6)$$

and $(\bar{G})^{-1}$ denotes the inverse matrix of \bar{G} .

In the Newton-Raphson iterative calculation, the initial values of the independent variables, \vec{x}^1 , are assumed before proceeding with the calculation. If \vec{f}^i is written for $\vec{f}(\vec{x}^i)$ and \bar{G}^i for the Jacobian matrix evaluated at \vec{x}^i , the values of the independent variables are repeatedly improved by

$$\begin{aligned}\vec{x}^{i+1} &= \vec{x}^i + \Delta \vec{x}^i \\ &= \vec{x}^i - (\bar{G}^i)^{-1} \vec{F}^i, \quad (i = 1, 2, \dots; i \text{ denotes the} \\ &\quad \text{iteration number}),\end{aligned}\quad (7)$$

until the following convergence criterion is satisfied :

$$J = \sum_{j=1}^n |f_j|/n < \text{convergence tolerance } (\epsilon). \quad (8)$$

In the Newton-Raphson method, initial estimation of the independent variables is a key step. If the initial estimates are far from the solutions, the iterative calculation usually fails to converge. On the other hand, even with fairly good estimates, divergence or great difficulty in achievement of convergence is often observed. In these cases, Eq.(7) must be replaced by the following special procedures.

2.1 Convergence Method 1

A coefficient, α^i ($0 < \alpha^i \leq 1$), is introduced and Eq.(7) is replaced by

$$\vec{x}^{i+1} = \vec{x}^i + \alpha^i \Delta \vec{x}^i. \quad (9)$$

α^i is determined so that J^{i+1} ($= \sum_{j=1}^n |f_j^{i+1}|/n$) is minimized at each iterative step. However, there is no single-variable optimization technique applicable to the cases where the unimodality is not inherent in J . For this reason, J^{i+1} is evaluated at a total of twenty different values of the coefficient :

$$\alpha_k^i = 0.05k, \quad (k = 1, \dots, 20), \quad (10)$$

and α_q^i which minimizes J^{i+1} is chosen and a set of the independent variables is determined for the next iterative step by

$$\vec{x}^{i+1} = \vec{x}^i + \alpha_q^i \Delta \vec{x}^i \quad (11)$$

2.2 Convergence Method 2

In this method, the maximum values of $|\Delta x_j|$ which are allowable at the iterative steps, δ_j , are prescribed before proceeding with the calculation. At every step, $|\Delta x_j^i|$ is checked if it exceeds δ_j or not. If $|\Delta x_j^i|$ is smaller than δ_j , the following is used :

$$x_j^{i+1} = x_j^i + \Delta x_j^i \quad , \quad (12)$$

but if it exceeds δ_j , the above equation is replaced by

$$x_j^{i+1} = x_j^i + \text{SIGN}(\delta_j, \Delta x_j^i) \quad , \quad (13)$$

where

$$\text{SIGN}(a, b) = \begin{cases} a & (b > 0) \\ -a & (b < 0) \end{cases} \quad , \quad (a > 0) \quad . \quad (14)$$

More difficulty in achievement of convergence requires smaller δ_j . In most cases, δ_j is required to be less than 10 % of x_j^1 .

2.3 Convergence Method 3

Although application of the previously described convergence methods are often successful, we still come across the cases where convergence is greatly difficult to achieve. In the third method, the procedure for determination of a new set of the independent variables is the same as that in the first one, with the exception of the following special modification. A set of coefficients, β_j 's ($0 < \beta_j \leq 1$), are prescribed in advance. At every iterative step, J^{i+1} is evaluated at α_k^i 's ($k = 1, \dots, 20$), but $|\alpha_k^i \Delta x_j^i|$ is checked before the evaluation if it exceeds $\beta_j x_j^i$ or not. If it is smaller than $\beta_j x_j^i$, the evaluation is made by using

$$x_j^{i+1} = x_j^i + \alpha_k^i \Delta x_j^i \quad (15)$$

If it exceeds $\beta_j x_j^i$, the following is used instead :

$$x_j^{i+1} = x_j^i + \text{SIGN}(\beta_j x_j^i, \alpha_k^i \Delta x_j^i) \quad (16)$$

α_q^i minimizing J^{i+1} and the corresponding \vec{x}^{i+1} are thus chosen for the next iterative step*. More difficulty in achievement of convergence requires smaller β_j . In most cases, β_j is required to be smaller than 0.1.

* x_j^{i+1} 's are determined by using Eqs.(15) and (16) where α_k^i is replaced by α_q^i .

3. Mathematical Simulation Procedure for Falling Liquid Film Condenser

For analysis of separation characteristics of the falling liquid film condenser, a hypothetical system as illustrated in Fig. 2 is considered as a model column. It is assumed that one feed stream exists at any stage except the first stage and the N-th stage. Basic equations are derived from the requirements for conservation of material and heat, and for phase equilibrium on any stage.

Component material balances ($i = 1, \dots, m$) :

$$\begin{aligned} V_2 y_{i,2} - V_1 y_{i,1} - L_1 x_{i,1} &= 0 , \\ L_{j-1} x_{i,j-1} + V_{j+1} y_{i,j+1} + F_j z_{i,j} - V_j y_{i,j} - L_j x_{i,j} &= 0 , \\ (j = 2, \dots, N-1), \\ L_{N-1} x_{i,N-1} - V_N y_{i,N} - L_N x_{i,N} &= 0 . \end{aligned} \quad (17)$$

Heat balances :

$$\begin{aligned} E_{1,in} = V_2 H_2 , \quad E_{1,out} = V_1 H_1 + L_1 h_1 + Q_1 , \\ E_{j,in} = L_{j-1} h_{j-1} + V_{j+1} H_{j+1} + F_j H_{Fj} , \\ E_{j,out} = L_j h_j + V_j H_j + Q_j , \\ E_j = 1 - E_{j,out}/E_{j,in} = 0 , \quad (j = 1, \dots, N-1). \end{aligned} \quad (18)$$

Vapor-liquid equilibrium :

$$y_{i,j} = K_{eqi,j} x_{i,j} , \quad (i = 1, \dots, m ; j = 1, \dots, N) . \quad (19)$$

Overall material balances :

$$L_j + V_1 - V_{j+1} - \sum_{k=1}^j F_k = 0 , \quad (j = 1, \dots, N-1 ; F_1 = 0) . \quad (20)$$

Overall heat balances :

$$\sum_{k=2}^j F_k H_{Fk} + H_{j+1} V_{j+1} = H_1 V_1 + h_j L_j + \sum_{k=1}^j Q_k , \quad (j = 1, \dots, N-1) . \quad (21)$$

The flow rate of the bottom product, B, is expressed by

$$E_N = 1 - B/L_N = 0 . \quad (22)$$

Substituting Eq.(19) into Eq.(17) yields the following tridiagonal matrix equations ($i = 1, \dots, m$) :

$$\begin{pmatrix} B_{i,1} & C_{i,1} & 0 & \dots & 0 \\ A_{i,2} & B_{i,2} & C_{i,2} & & \\ \dots & \dots & \dots & & \\ & A_{i,j} & B_{i,j} & C_{i,j} & \\ & & \dots & \dots & \\ & & & A_{i,N-1} & B_{i,N-1} & C_{i,N-1} \\ 0 & \dots & 0 & A_{i,N} & B_{i,N} \end{pmatrix} \begin{pmatrix} x_{i,1} \\ x_{i,2} \\ \vdots \\ x_{i,j} \\ \vdots \\ x_{i,N-1} \\ x_{i,N} \end{pmatrix} = \begin{pmatrix} D_{i,1} \\ D_{i,2} \\ \vdots \\ D_{i,j} \\ \vdots \\ D_{i,N-1} \\ D_{i,N} \end{pmatrix} , \quad (23)$$

where

$$\begin{aligned} B_{i,1} &= -(L_1 + V_1 K_{eqi,1}), & C_{i,1} &= V_2 K_{eqi,2}, & D_{i,1} &= 0, \\ A_{i,j} &= L_{j-1}, & B_{i,j} &= -V_j K_{eqi,j} - L_j, \\ C_j &= V_{j+1} K_{eqi,j+1}, & D_j &= -F_j z_{i,j}, & (j=2, \dots, N-1), \\ A_{i,N} &= L_{N-1}, & B_{i,N} &= V_N K_{eqi,N} - L_N, & D_N &= 0 . \end{aligned}$$

If L_j 's and T_j 's are known, V_j 's and $K_{eqi,j}$'s can be calculated in cases where $K_{eqi,j}$ is independent of liquid composition, and the liquid mole fractions can be determined by solving Eq.(23) m times, followed by normalization of $x_{i,j}$:

$$x_{i,j} := x_{i,j} / \sum_{i=1}^m x_{i,j} . \quad (24)$$

If the feed conditions, top gas flow rate, number of total theoretical stages, operating pressure and amount of heat subtracted on any stage are all specified, distributions of temperature, liquid and gas flows and compositions of the two phases can be calculated by finding out the solutions of the following $2N$ -dimensional nonlinear simultaneous equations (3):

$$\left. \begin{aligned} S_1(T_1, \dots, T_N, L_1, \dots, L_N) &= 0 \\ &\vdots \\ S_N(T_1, \dots, T_N, L_1, \dots, L_N) &= 0 \\ E_1(T_1, \dots, T_N, L_1, \dots, L_N) &= 0 \\ &\vdots \\ E_N(T_1, \dots, T_N, L_1, \dots, L_N) &= 0 \end{aligned} \right\} , \quad (25)$$

where S_j is defined by

$$S_j = \sum_{i=1}^m K_{eqi,j} x_{i,j} - 1. \quad (26)$$

Equation (25) is solved by application of the multi-dimensional Newton-Raphson method which was explained in the previous chapter.

As emphasized before, initial estimation of the independent variables (L_j 's and T_j 's) is a key procedure. For initial

estimation of temperatures, the three temperatures, T_1 , T_2 and T_N , are first assumed, and then the other temperatures are determined by interpolation by using the assumption of linear functions of the number of the theoretical stages. Since both the liquid and gas flows increase remarkably in the cooled section as the stage number increases, the usual assumption of the equal molal overflows for initial estimation of liquid flows, always fails to converge. In the present procedure, initial estimation of phase flows is made as described below.

- 1) Assume the composition profiles within the column. One of the possible methods for the column with a single feed is expressed by

$$x_{i,j} := z_{i,N_F}, \quad y_{i,j} := z_{i,N_F},$$

$$(i = 1, \dots, m; j=1, \dots, N). \quad (27)$$

- 2) Calculate the liquid enthalpies h_j 's and gas enthalpies H_j 's.
- 3) Calculate the liquid flow rates L_j 's ($j = 1, \dots, N-1$) from

$$L_j = \{ (H_1 - H_{j+1})V_1 + \sum_{k=1}^j Q_k - \sum_{k=1}^j F_k H_{Fk} + H_{j+1} \sum_{k=1}^j F_k \} /$$

$$(H_{j+1} - h_j), \quad (j = 1, \dots, N-1; F_1 = 0). \quad (28)$$

This equation is obtained by substitution of Eq.(20) into Eq.(21).

- 4) Calculate the gas flow rates V_j 's ($j = 2, \dots, N$) from Eq.(20).

Once the initial estimation is made, the values of the independent variables are repeatedly improved by using one of the convergence methods previously described until the following convergence criterion is satisfied :

$$J = \left\{ \sum_{j=1}^N (|S_j| + |E_j|) \right\} / (2N) < \text{convergence tolerance } (\epsilon). \quad (29)$$

In the simulation, the total of seven components should be considered : ${}^4\text{He}$ and the six isotopic species of molecular hydrogen. Although the data on vapor-liquid equilibrium of the seven component system is not available, Sherman⁽⁴⁾ measured the equilibrium relationships for the three systems, H_2 - ${}^4\text{He}$ system, D_2 - ${}^4\text{He}$ and T_2 - ${}^4\text{He}$. In the present study, the vapor-liquid equilibrium ratio of each component is estimated as described below. For the six molecular species, the following postulation known as the Raoult's law is made :

$$y_{i,j} P_j = p_{i,j}^{\circ} x_{i,j} \quad (30)$$

For ${}^4\text{He}$, the following equation is used :

$$y_{\text{He},j} P_j = c_{\text{He},j} x_{\text{He},j} \quad (31)$$

where the coefficient $c_{\text{He},j}$ is calculated from the Henry's constants of the three systems ($c_{\text{He-H}_2}$, $c_{\text{He-D}_2}$ and $c_{\text{He-T}_2}$) by using

$$\left. \begin{aligned} c_{\text{He},j} &= \sum_{i=1}^6 c_{\text{He}-i,j} x'_{i,j} \\ x'_{i,j} &= x_{i,j} / \sum_{i=1}^6 x_{i,j} \end{aligned} \right\} \quad (32)$$

$$\left. \begin{aligned}
 c_{\text{He-HD},j} &= \sqrt{c_{\text{He-H}_2,j} c_{\text{He-D}_2,j}} \\
 c_{\text{He-HT},j} &= \sqrt{c_{\text{He-H}_2,j} c_{\text{He-T}_2,j}} \\
 c_{\text{He-DT},j} &= \sqrt{c_{\text{He-D}_2,j} c_{\text{He-T}_2,j}}
 \end{aligned} \right\} \quad (33)$$

Since Souers⁽⁵⁾ proposes the expression for $c_{\text{He-}i,j}$,

$$c_{\text{He-}i,j} = a_i \text{EXP}(b_i / T_j) , \quad (34)$$

the coefficients, a_i 's and b_i 's, are determined so that the calculated values fit Sherman's experimental data :

$$\left. \begin{aligned}
 a_{\text{H}_2} &= 4.39 \quad , \quad b_{\text{H}_2} = 94.6 \\
 a_{\text{D}_2} &= 9.16 \quad , \quad b_{\text{D}_2} = 108.6 \\
 a_{\text{T}_2} &= 18.0 \quad , \quad b_{\text{T}_2} = 114.3
 \end{aligned} \right\} \quad (35)$$

Henry's constants are assumed to be independent of total pressure. $C_{\text{He},j}$ depends not only upon temperature but also upon liquid composition. This requires an additional iteration loop, because the vapor-liquid equilibrium ratio in Eq.(19) must be independent of liquid composition. In the present procedure, the successive iteration method is applied for the outer iteration loop (the inner iteration loop is the Newton-Raphson calculation), as illustrated in Fig. 3. The initial values of the liquid mole fractions are assumed to be equal to the feed mole fractions for the outer loop. The effects of the uncertainties of the experimentally determined parameters are explored later to support the conclusions.

4. Separation Characteristics

4.1 Distributions of Temperature, Phase Flows and Compositions

In order to analyze the distributions of the column variables such as temperatures, liquid and gas flows and compositions of the two phases, the feed specifications and the calculational conditions are assumed as given in Tables 1 and 2, respectively. The calculation is made by using the simulation model described in the previous chapter. The distributions of temperature and phase flows are summarized in Table 3. The composition profiles are shown for representative components in Figs. 4 and 5.

It is observed from Table 3 that as the stage number increases, the liquid and gas flows increase remarkably in the cooled section while they are almost unchanged in the packed section. The temperature on the first stage is exceptionally low in comparison to the other temperatures. The predominant isotopic species of molecular hydrogen in the top gas are H_2 and HD. The recovery fraction of tritium to the bottom exceeds 99.9 %. The bottom liquid is almost completely free from helium (helium concentration ~ 0.01 ppm).

4.2 Effect of Operating Pressure

It is desired that the percentage of hydrogen isotopes contained in the top gas be reduced to be as few as possible. However, a lower percentage is expected to cause lower gas temperature and further lower inlet temperature of the refrige-

rant. This conflicts with the need that the inlet temperature be sufficiently high to prevent hydrogen isotopes from freezing. The key parameter to solve this problem is the operating pressure. For this reason, a parametric survey is made for P changing the two parameters, P and V_1 . These two parameters are established so that the temperature of the first stage T_1 remains almost constant. The effect of the operating pressure is summarized in Table 4 and Fig. 6. The percentage of hydrogen isotopes in the top gas decreases greatly with increase in P in the range of low pressure. However, this parameter remains almost unchanged in the high pressure range. It may be concluded that the optimum pressure lies in the range from 4 atm to 5 atm. The percentage of hydrogen isotopes in the top gas can be kept approximately 10 mol%. It should be noted that this percentage is almost independent of parameters other than the operating pressure.

4.3 Convergence Characteristics

The convergence parameters which could have substantial influence on convergence characteristics of the Newton-Raphson iterative calculation are T_1^0 , T_2^0 and T_N^0 for initial estimation of a set of temperatures, δ_j 's in the second convergence method and β_j 's in the third one if these methods are used. Unfortunately, there are no methods available which allow us to predict the best method for convergence or optimum set of these convergence parameters. Table 5 summarizes the convergence methods and parameters used in calculations and informa-

tion on convergence characteristics observed, for several representative cases. The three temperatures for initial estimates have profound effects on achievement of convergence. The higher operating pressure results in more difficulty in achievement of convergence, which requires application of special convergence methods. As an example, Fig. 7 shows the graph of J (Eq.(29)) plotted against the iteration number. The number of iterations needed for the outer successive iteration loop is three and that of the total iterations is thirteen. The conclusion is that convergence of the calculation is often difficult to achieve, but it can be ensured by pertinent establishment of the convergence parameters.

4.4 Effects of Number of Total Packed Stages and Total Amount of Heat Subtracted

One of the most attractive features of the falling liquid film condenser is promotion of separation of hydrogen isotopes by using the packed section. If attention is focused on removal of helium, even small values of the number of the total packed stages and total amount of heat subtracted from the cooled section, are quite satisfactory. However, the tritium concentration in the top gas should be considered a key output parameter. Figure 8 shows the effect of the number of total packed stages on this key parameter. In all the cases in Fig. 8, the number of the total cooled section is fixed at 15 and the amount of heat subtracted is also unchanged (= 1000 cal/h/stage). The feed stage number, N_F , is equal to $N-2$. If the feed is

supplied to a point higher, the helium concentration in the bottom liquid will be greatly decreased, but it is already extremely low and the low tritium concentration in the top gas should be considered more important. Figure 8 indicates that the tritium concentration in the top gas can be decreased to almost unlimited extent by increasing the packed height. The tritium concentration in the top gas can also be decreased by providing larger amount of heat subtracted from the cooled section. This is observed in Table 6. Another information learned from this table is that helium concentration in the bottom liquid is also decreased by larger amount of heat subtracted, while it remains almost unchanged with increase in the packed height.

Importance of the three temperatures assumed for the initial estimation of a set of temperatures, can be appreciated in the calculation of Case 9. With the three temperatures of 20.0 K, 27.5 K and 30.0 K, the calculation converged in 15 iterations (Method 3, β_j 's are 0.05 for L_j 's and 0.005 for T_j 's), but it failed to converge in 50 iterations if 30.0 K was changed to 30.5 K.

4.5 Discussion on Uncertainty of Volatility of Helium

Although detailed information on column behavior is obtained by the parametric studies made in the previous sections, the parameters experimentally determined for calculation of the equilibrium ratio for helium are more or less uncertain. For this reason, two calculations are added changing a 's in Eq.(35) under the reference condition. One calculation is made by

doubling a's and the other by halving a's. The results indicate that all the column variables remain almost unchanged except the helium concentration in liquid phases. The calculated values of the helium concentration in the bottom liquid are approximately 0.001 ppm and 0.1 ppm, respectively. However, the helium concentration in the bottom liquid is always sufficiently low, and uncertainty of the experimentally determined parameters is not significant.

4.6 Addition of Protium to Feed Stream

The bottom stream from the falling liquid film condenser is transferred to the cryogenic distillation column cascade for hydrogen isotope separation. One of the features of the column cascade is that the top flow of H_2 and HD from Column(2) is considerably small (~ 0.3 g-mol/h).⁽⁶⁾ If the falling liquid film condenser is incorporated between the fuel clean-up system and the column cascade, the top flow from Column(2) is further decreased because a significant percentage of protium is removed by the falling liquid film condenser. For this reason, it may be profitable to add protium to the feed stream supplied to the falling liquid film condenser, for ensurance of the adequate flow from the top of Column(2). An additional calculation reveals that it also results in reduction of the tritium concentration in the top gas from the falling liquid film condenser. If the protium percentage is doubled in Reference Case with the other conditions unchanged, for instance, the atom percentage of tritium decreases to 0.0869 %.

5. Conclusion

- (1) A falling liquid film condenser is proposed as a most attractive process for removal of helium from hydrogen isotopes. A condenser is composed of a cooled section of a tapered column and a packed section. The feed is supplied to a point near the lower end of the packed section.
- (2) A mathematical simulation procedure is developed for analyses on separation characteristics of the column. A total of seven components (He, H₂, HD, HT, D₂, DT and T₂) are considered in the simulation model. It is verified that the convergence is ensured in a wide range of conditions by appropriate establishment of the convergence parameters.
- (3) The percentage of hydrogen isotopes in the top gas can be kept about 10 % with the operating pressure of ~ 5 atm. A sufficiently long packed section ensures considerably low tritium concentration in the top gas (lower than 0.01 atom%). The top gas can be transferred to the tritium waste treatment system. The liquid hydrogen isotopes withdrawn from the bottom of the column is almost completely free from helium (helium concentration ~ 0.01 ppm).
- (4) It is desired that dynamic simulation studies or exploration of control systems be made in further studies. The key output parameter to be controlled is the tritium concentration in the top gas.

NOMENCLATURE

- B : Prescribed value of L_N (g-mol/h)
 $c_{\text{He-i,j}}$: Henry's constant of He-i system at T_j K (atm)
 F_j : Flow rate of feed stream supplied to j-th stage (g-mol/h)
 H_j : Molal enthalpy of gas stream leaving j-th stage (cal/g-mol)
 H_{Fj} : Molal enthalpy of feed stream supplied to j-th stage
 (g-mol/h)
 h_j : Molal enthalpy of liquid stream leaving j-th stage
 (g-mol/h)
 $K_{\text{eqi,j}}$: Vapor-liquid equilibrium ratio of component i at T_j K
 L_j : Flow rate of liquid stream leaving j-th stage (g-mol/h)
 m : Total number of components
 N : Number of total theoretical stages
 N_F : Feed stage number
 P_j : Total pressure on j-th stage (atm)
 $p_{i,j}^{\circ}$: Vapor pressure of pure component i at T_j K (atm)
 Q_j : Amount of heat subtracted on j-th stage (cal/h)
 T_j : Absolute temperature on j-th stage (K)
 V_j : Flow rate of gas stream leaving j-th stage (g-mol/h)
 $x_{i,j}$: Mole fraction of component i in liquid stream leaving
 j-th stage
 $y_{i,j}$: Mole fraction of component i in gas stream leaving
 j-th stage
 $z_{i,j}$: Mole fraction of component i in feed stream supplied to
 j-th stage

ϵ : Convergence tolerance for inner iteration loop

μ : Convergence tolerance for outer iteration loop

(Subscript)

i : Component number

1 : H₂ , 2 : HD , 3 : HT , 4 : D₂ , 5 : DT , 6 : T₂ ,
7 : He .

j : Stage number

REFERENCES

- (1) Kinoshita, M., Bartlit, J. R., and Sherman, R. H. :
Private Communication, (1981), Japan Atomic Energy Research
Institute.
- (2) Kinoshita, M., Bartlit, J. R., and Sherman, R. H. :
Proceedings of 9-th Symposium on Engineering Problems of
Fusion Research, to be published.
- (3) Tomich, J. F. : AIChE J., 16, 229 (1970).
- (4) Souers, P. C. : UCRL-52628, 41 (1979).
- (5) Sherman, R. H. : Private Communication, (1981), Los Alamos
National Laboratory.
- (6) Bartlit, J. R., Sherman, R. H. : Private Communication,
(1981), Los Alamos National Laboratory.

ACKNOWLEDGMENT

The authors wish to express their sincere thanks to Dr. J. E. Baublitz (DOE), Dr. J. L. Anderson (LANL), Dr. Y. Obata (JAERI) and Mr. Y. Naruse (JAERI) for supporting the present study.

REFERENCES

- (1) Kinoshita, M., Bartlit, J. R., and Sherman, R. H. :
Private Communication, (1981), Japan Atomic Energy Research
Institute.
- (2) Kinoshita, M., Bartlit, J. R., and Sherman, R. H. :
Proceedings of 9-th Symposium on Engineering Problems of
Fusion Research, to be published.
- (3) Tomich, J. F. : AIChE J., 16, 229 (1970).
- (4) Souers, P. C. : UCRL-52628, 41 (1979).
- (5) Sherman, R. H. : Private Communication, (1981), Los Alamos
National Laboratory.
- (6) Bartlit, J. R., Sherman, R. H. : Private Communication,
(1981), Los Alamos National Laboratory.

ACKNOWLEDGMENT

The authors wish to express their sincere thanks to Dr. J. E. Baublitz (DOE), Dr. J. L. Anderson (LANL), Dr. Y. Obata (JAERI) and Mr. Y. Naruse (JAERI) for supporting the present study.

Table 1 Feed condition chosen for parametric studies

Composition	$H_2 = 0.013 \%$ $HD = 0.995 \%$ $HT = 0.879 \%$ $D_2 = 23.57 \%$ $DT = 45.91 \%$ $T_2 = 23.63 \%$ $He = 5.00 \%$
Flow rate	15.0 g-mol/h
State	Gas

The present study deals with a column with a single feed.

Table 2 Reference Case for parametric studies

Number of total theoretical stages = 30
Cooled section = Stages 1 through 15
Packed section = Stages 16 through 29
Feed stage number = 28
Flow rate of top gas = 0.85 g-mol/h
Operating pressure = 4 atm
Heat subtracted = 1000 cal/h/stage
Feed temperature = 30.5 K

Table 3 Distributions of temperature, gas flow rate,
and liquid flow rate within column in
Reference Case

j	T_j (K)	V_j (g-mol/h)	L_j (g-mol/h)
1	19.87	0.85	3.64
2	27.13	4.49	8.18
3	27.62	9.03	12.7
4	27.80	13.5	17.1
5	27.91	17.9	21.4
10	28.36	39.1	42.2
15	28.99	57.7	60.2
16	29.12	61.1	59.5
20	29.53	58.4	57.0
25	29.87	56.0	54.8
28	30.03	55.0	53.7
29	30.13	39.5	53.6
30	30.17	39.5	14.15

j : Stage number

T_j : Temperature on j-th stage

V_j : Flow rate of gas stream leaving j-th stage

L_j : Flow rate of liquid stream leaving j-th stage

Table 4 Effect of operating pressure on percentage of hydrogen isotopes in top gas

Case	P	V_1	H	T_1
1	1	1.15	34.8	19.9
2	2	0.95	21.1	19.9
3	3	0.885	15.3	19.9
Reference	4	0.85	11.8	19.9
4	5	0.83	9.64	19.9

P : Operating pressure (atm)

V_1 : Flow rate of top gas (g-mol/h)

H : Percentage of hydrogen isotopes in top gas (%)

T_1 : Temperature of top gas (K)

Feed temperatures assumed are as follows :

24.5 K (Case 1), 27.5 K (Case 2), 29.0 K (Case 3),

30.5 K (Reference Case), 31.5 K (Case 4).

Table 5 Information on convergence characteristics

Case	T_1^0	T_2^0	T_N^0	Method	n
1	20.0	23.0	24.5	0	7
2	20.0	25.0	27.0	0	divergence
2	20.0	25.0	27.0	1	11
Reference	20.0	27.5	30.5	1	divergence
Reference	20.0	27.5	30.5	3	13*
Reference	20.0	27.5	30.5	3	11**
Reference	20.0	25.0	30.5	3	nonconvergence*
4	20.0	28.5	31.5	3	14*

T_j^0 : Temperatures chosen for initial estimation of a set of temperatures (K)

Method : Convergence method selected (Method 0 means the normal Newton-Raphson method without any special consideration)

n : Number of total iterations needed

divergence : The calculation was abnormally terminated because infinitively large numbers appeared.

nonconvergence : The calculation did not converge in 50 iterations.

* β_j 's are 0.05 for liquid flows and 0.005 for temperatures.

** β_j 's are 0.1 for liquid flows and 0.01 for temperatures.

Once the inner iterative calculation converge, the outer one never fails to converge.

Table 6 Effects of number of total packed stages and total amount of heat subtracted

Case	N	N _F	Q _j	T ₁	C _T	C _{He}
6	20	18	1000	20.2	0.649	0.01
Reference	30	28	1000	19.9	0.282	0.01
7	50	48	1000	19.8	0.0195	0.01
8	30	28	700	19.9	0.448	0.02
9	30	28	1500	19.8	0.211	0.005

Cooled section = Stages 1 through 15

Operating pressure = 4 atm

N : Number of total theoretical stages N_F : Feed stage number

Q_j : Amount of heat subtracted (cal/h/stage) T₁ : Temperature on first stage (K)

C_T : Tritium percentage in top gas (atom%) C_{He} : Helium concentration in bottom liquid (ppm)

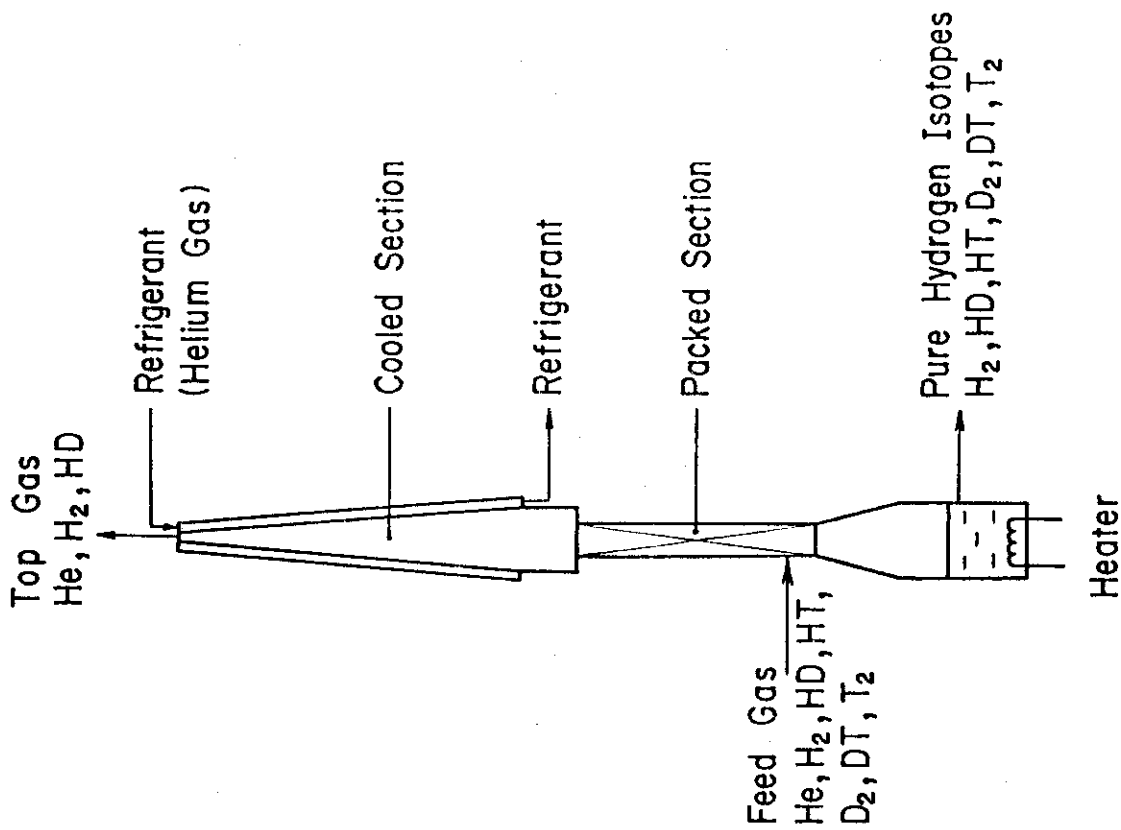


Fig. 1 Conceptual flow diagram of falling liquid film condenser

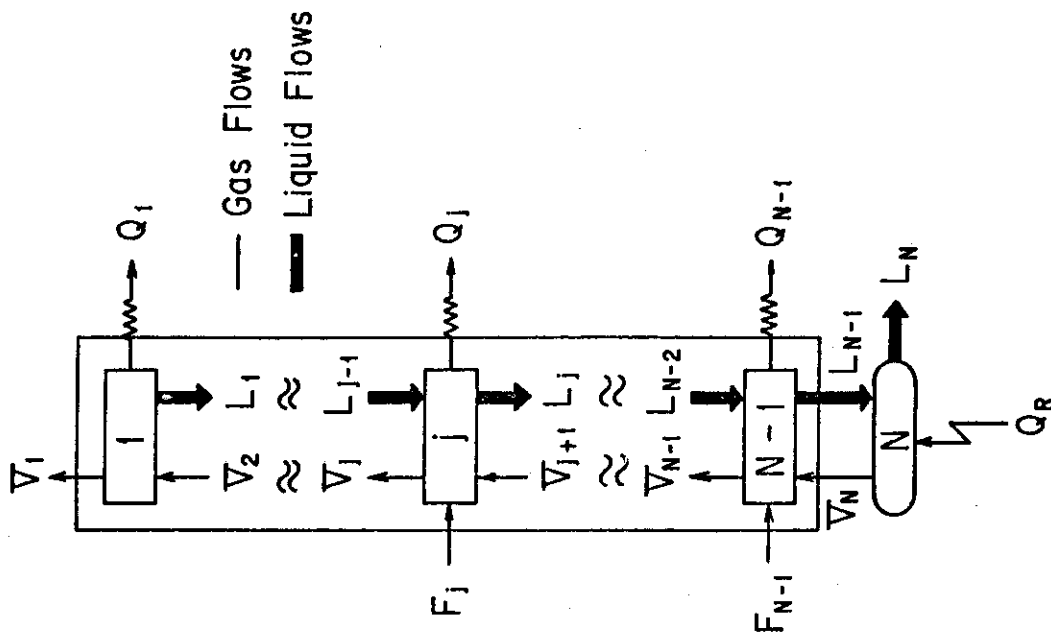


Fig. 2 Model column for mathematical simulation

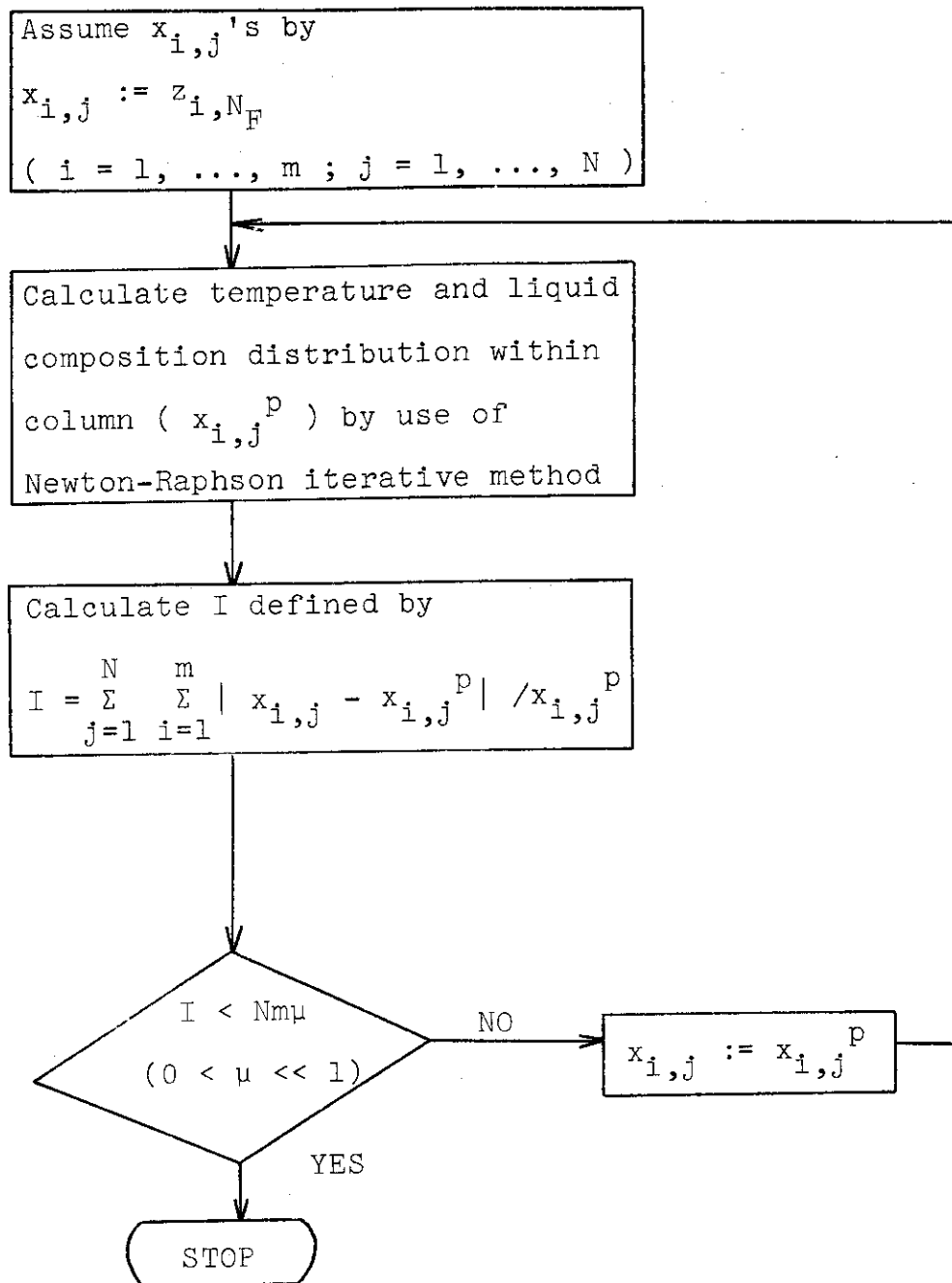


Fig. 3 Outer iterative loop (successive iteration)
in mathematical simulation

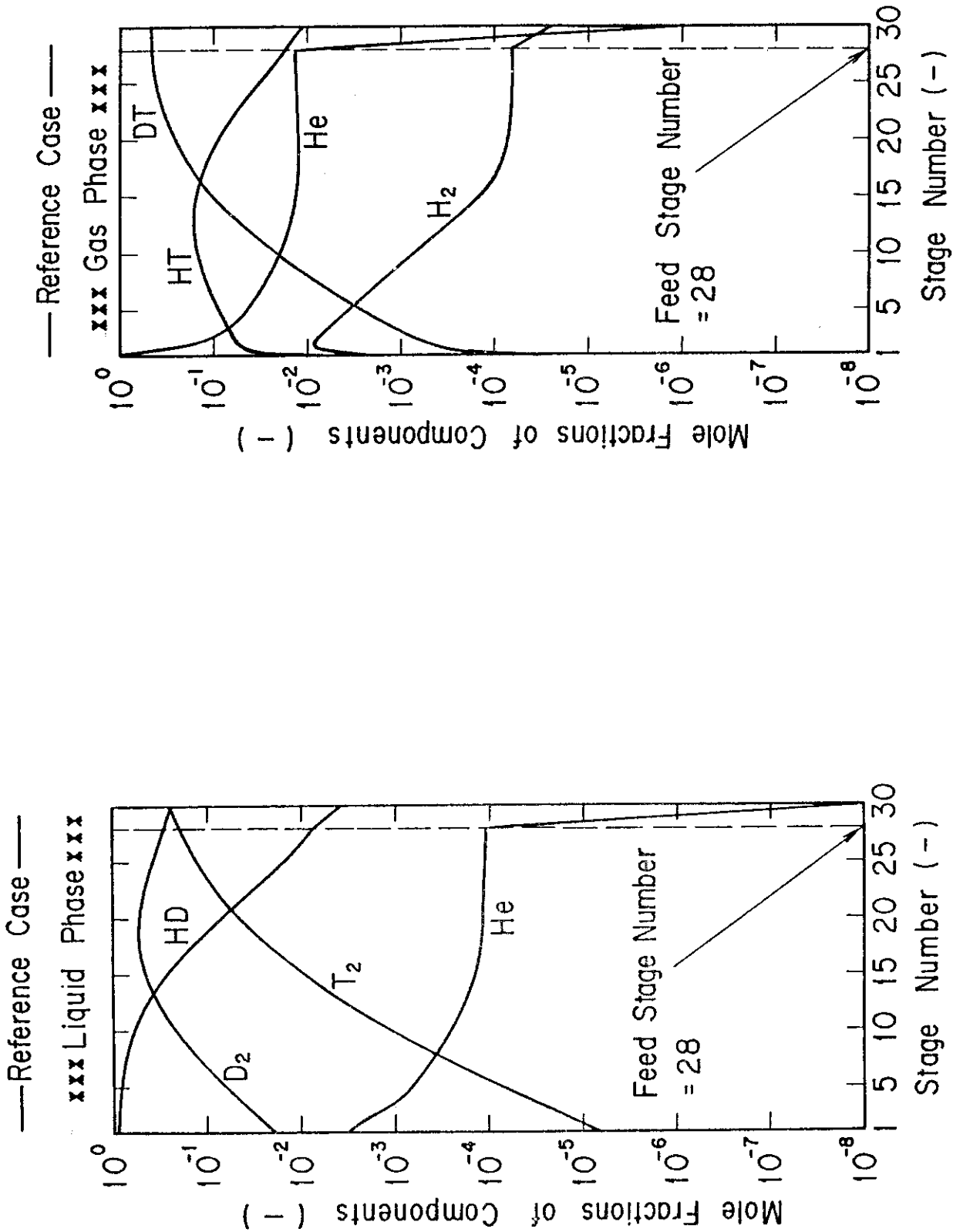


Fig. 4 Example of liquid composition distribution for representative components within column

Fig. 5 Example of gas composition distribution for representative components within column

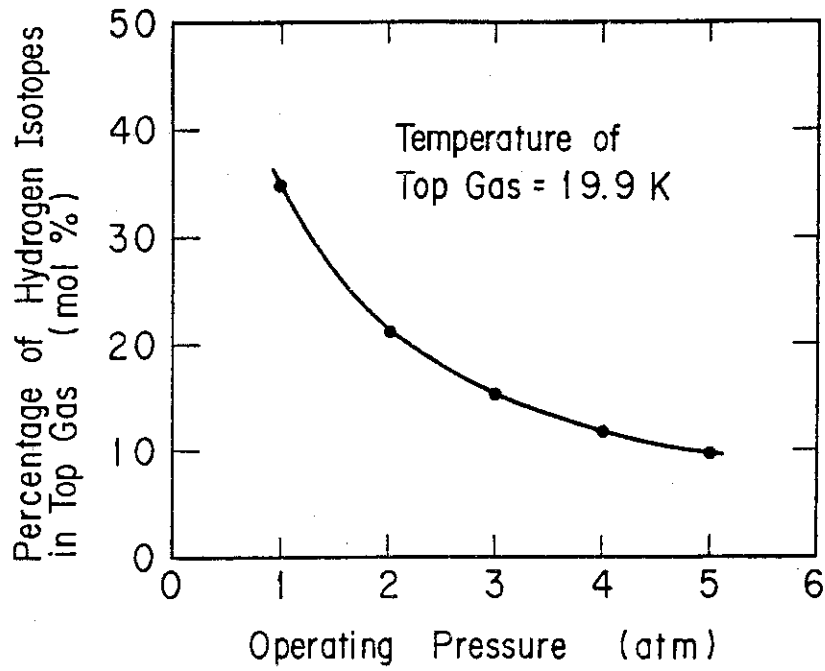


Fig. 6 Effect of operating pressure on percentage of hydrogen isotopes in top gas

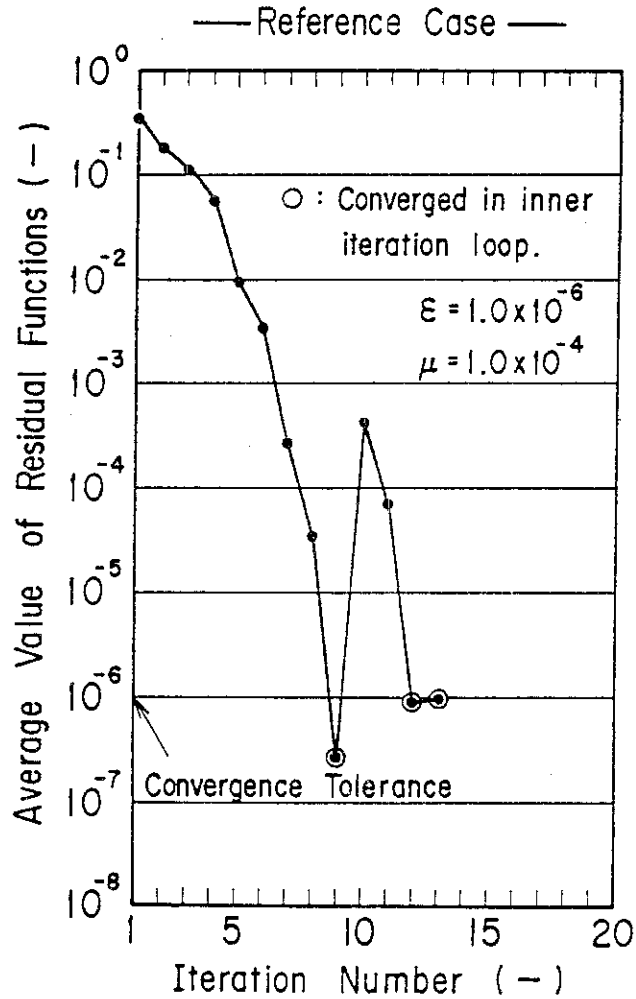


Fig. 7 Example of successful achievement of convergence

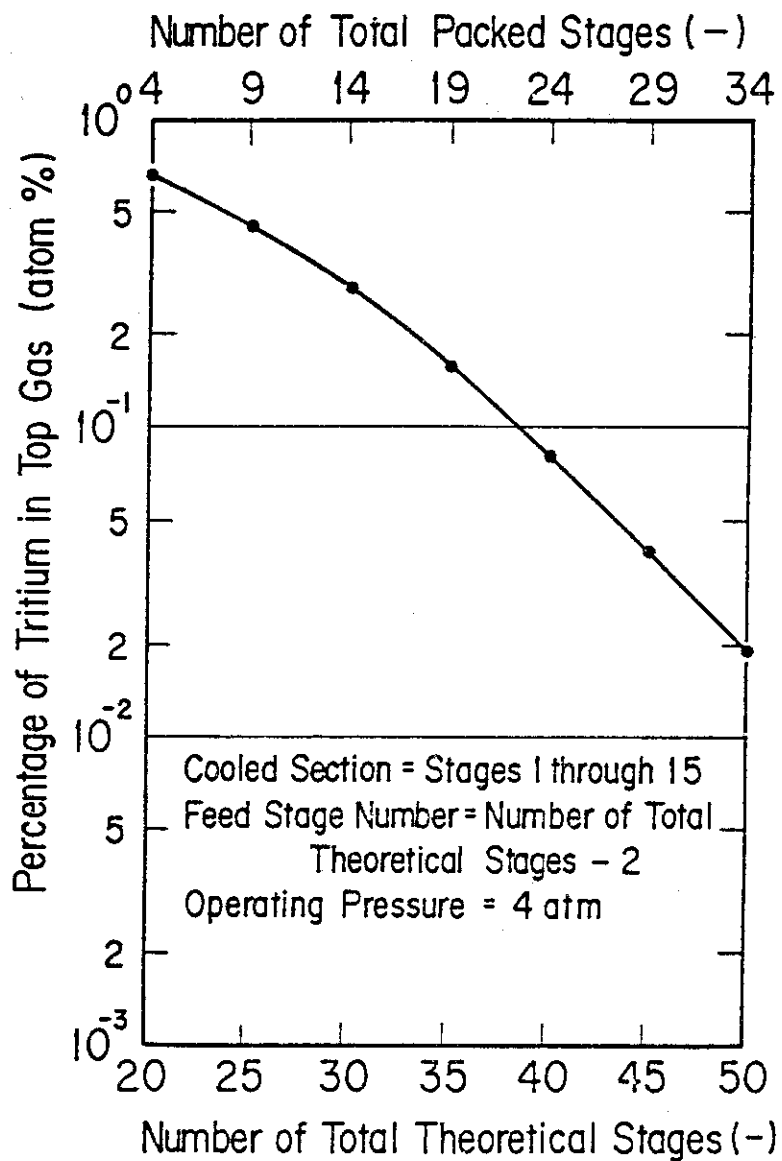


Fig. 8 Effect of number of total packed stages on tritium percentage in top gas